Low energy electron scattering from CO: absolute cross section measurements and ***R***-matrix calculations

1996 J. Phys. B: At. Mol. Opt. Phys. 29 3197

(http://iopscience.iop.org/0953-4075/29/14/026)

J. Phys. B: At. Mol. Opt. Phys. **29** (1996) 3197–3214. Printed in the UK

Low energy electron scattering from CO: absolute cross section measurements and *R*-matrix calculations

Jennifer C Gibson†, Lesley A Morgan‡, Robert J Gulley§, Michael J Brunger‖, Christoph T Bundschu† and Stephen J Buckman†

† Atomic and Molecular Physics Laboratories, Research School of Physical Sciences and Engineering, Australian National University, Canberra, ACT, Australia
‡ Computer Centre, Royal Holloway, University of London, Egham, Surrey, UK
§ CLRC, Daresbury Laboratory, Warrington, UK
‖ Physics Department, Flinders University of South Australia, Bedford Park, SA, Australia

Received 9 January 1996

Abstract. Absolute cross sections for elastic scattering and rovibrational excitation have been measured with a crossed beam spectrometer and calculated, utilizing the *R*-matrix formalism, for incident electron energies between 1.0 and 30 eV. Particular emphasis is placed on the comparison between experiment and theory in the region below 5 eV where the cross sections are enhanced by a strong $^2\Pi$ shape resonance.

1. Introduction

The understanding of the low energy electron scattering cross sections for CO has assumed significance in recent times because of the importance of this molecule in our own atmosphere and the interstellar medium, and the role that it plays in a wide variety of gas discharge processes. It is also an interesting theoretical challenge in that it offers the relative simplicity of a reasonably small, closed shell molecule which is weakly polar and which is known to exhibit strong shape resonance effects at low incident energies, particularly in the vibrational excitation channels. In addition it is isolelectronic with N_2 and a number of previous studies have highlighted the similarities in the shape and magnitude of the elastic differential cross sections (DCS) for the two gases (e.g. Nickel *et al* 1988, Middleton *et al* 1992).

Previous experimental electron scattering work on CO is extensive although, somewhat surprisingly, it is characterized by a lack of recent, absolute differential cross section measurements at energies below about 5 eV. Previous relevant measurements which cover the current energy range of interest (1–30 eV) include the relative angular distributions for elastic scattering and vibrational excitation of Ehrhardt *et al* (1968), the elastic DCS measurements of Tanaka *et al* (1978), the vibrational excitation DCS of Chutjian and Tanaka (1980) and Tronc *et al* (1980), the elastic and vibrational cross sections of Jung *et al* (1982), the rotational excitation cross sections of Sohn *et al* (1985) and Gote and Ehrhardt (1995), the elastic DCS measurements of Nickel *et al* (1988) and the vibrational excitation cross sections and elastic and electronic excitation measurements of Middleton *et al* (1992, 1993). There have been a substantial number of measurements of the grand total cross section in recent years but rather than list them all here we refer to the recently published

0953-4075/96/143197+18$19.50

'recommended' cross section of Kanik *et al* (1993) which contains a comprehensive list of references to previous work. Theoretical interest in this problem has been fragmentary, due in some part to the difficulties which the long-range dipole interaction poses for calculations formulated in the fixed-nuclei approximation. Onda and Truhlar (1980) calculated elastic DCS in a close coupling approach with a self-consistent field (SCF) treatment of polarization and a local exchange approximation. DCS calculations for both elastic scattering and vibrational excitation using the *R*-matrix approach have been reported by Morgan (1991) and Morgan and Tennyson (1993) and integral cross sections by Salvini *et al* (1984). Jain and Norcross (1992) have used an exact exchange plus parameter-free polarization model to calculate both rotationally elastic and inelastic DCS and integral cross sections between 0.001 and 10 eV.

The present work is intended to provide an extensive set of absolute DCS for elastic scattering and vibrational (0–1) excitation from the ground $X\,^1\Sigma_g^+$ state between 1 and 30 eV, to enable critical comparison with recent *R*-matrix calculations and other experiments, particularly those below 5 eV incident energy. The experimental method and theoretical treatment are discussed briefly and extensive comparisons are provided between various experiments and theory at both the differential and integral cross section level.

2. Experimental apparatus and procedures

The present experiments have been carried out using a crossed electron–molecular beam apparatus. This apparatus has been described in substantial detail in previous papers (Brunger *et al* 1990, Gulley *et al* 1994) and so we will only provide a brief discussion of the relevant experimental details here. The electron beam, produced by a combination of electrostatic electron optical elements and a hemispherical monochromator, crosses the gas beam formed by quasi-effusive flow from a multicapillary array. Scattered electrons, either elastic or those that have lost 0.266 eV in exciting the 0–1 vibrational mode of the CO $X\,^1\Sigma_g^+$ ground state, are transported, analysed and detected by a similar electrostatic analyser and channel electron multiplier detector. The overall energy resolution of the spectrometer for these measurements was typically 50 meV and the beam current delivered to the interaction volume was between 0.5 and 2 nA, depending on the beam energy. The scattered electrons can be detected over an angular range of -15° to 130° by rotating the analyser about the molecular beam axis. The energy scale was established by calibration measurements in N_2 using the position of the second quasi-vibrational resonance peak in the elastic scattering channel as a reference. The energy of this structure, at a scattering angle of 60°, was taken to be 2.198 eV Rohr (1977).

As in past measurements with this apparatus, particular attention has been paid to the conditions under which the molecular beam is formed. This was necessary to ensure the correct application of the relative flow technique (e.g. Nickel *et al* 1989, Buckman *et al* 1993) which is used to place the relative angular distributions on an absolute scale. This technique involves the measurement of ratios of scattered signal between the gas of interest and a reference or 'standard' gas, usually helium. It is therefore imperative that these measurements be carried out under identical conditions, particularly with regard to the size of the interaction volume. In the present case this is achieved by a number of measures. Firstly, the two gases under study, CO and He, are both present in the scattering chamber at all times so that gas cycling does not have an effect on the energy, spatial dimensions or magnitude of the electron beam. Secondly, the driving pressures of the two gases, measured at the entrance to the capillary array, are chosen such that their mean free paths are identical. These pressures are determined by calculations based on molecular diameters

Table 1. Absolute differential cross sections (10^{-16} cm^2 sr^{-1}) for elastic electron scattering from CO: (*a*) in the region of the $^2\Pi$ resonance; (*b*) between 5 and 30 eV. Numbers in parentheses indicate the absolute uncertainty of the present measurements expressed as a percentage. Integral elastic (σ_E) and momentum transfer (σ_M) cross sections are given in units of 10^{-16} cm^2 with an estimated uncertainty of ±15%.

(*a*)	Energy (eV)					
Angle	1.0	1.25	1.50	1.91	2.45	3.0
15			3.362 (7)	5.974 (7)	5.389 (7)	3.789 (7)
17		1.370 (9)				
20		1.260 (7)	3.041 (6)	5.757 (7)	5.267 (7)	3.853 (7)
25	0.591 (14)		2.733 (7)	5.510 (8)	5.318 (7)	3.917 (7)
30	0.542 (7)	0.967 (7)	2.526 (6)	5.232 (8)	5.097 (7)	3.846 (7)
35			2.294 (7)	4.928 (8)	4.980 (7)	3.745 (7)
40	0.480 (7)	0.831 (7)	2.073 (7)	4.619 (8)	4.625 (7)	3.600 (7)
45			1.937 (6)	4.285 (7)	4.392 (7)	3.407 (7)
50	0.540 (6)	0.804 (7)	1.841 (7)	3.951 (8)	4.018 (7)	3.190 (7)
55			1.745 (6)	3.560 (9)	3.742 (7)	2.953 (7)
60	0.670 (6)	0.884 (6)	1.677 (6)	3.278 (7)	3.364 (7)	2.651 (7)
70	0.850 (6)	1.048 (7)	1.659 (6)	2.789 (7)	2.956 (7)	2.144 (7)
80	1.041 (7)	1.219 (7)	1.741 (6)	2.329 (7)	2.287 (7)	1.619 (7)
90	1.240 (7)	1.430 (6)	1.827 (6)	2.000 (7)	1.575 (7)	1.228 (7)
100	1.415 (6)	1.603 (7)	1.937 (6)	1.716 (7)	1.180 (7)	0.916 (7)
110	1.573 (6)	1.761 (6)	2.055 (6)	1.551 (7)	0.924 (7)	0.720 (7)
120	1.701 (6)	1.920 (6)	2.219 (6)	1.506 (7)	0.822 (7)	0.621 (7)
130	1.802 (6)	2.078 (6)	2.445 (6)	1.634 (7)	0.880 (7)	0.674 (7)
σ_E	15.4	20.4	26.8	35.8	30.2	22.7
σ_M	19.1	25.4	27.8	30.1	21.4	15.8

for these gases of 3.690 Å (CO) and 2.551 Å (He) (Reid *et al* 1987). Thirdly, the driving pressures are chosen such that the mean free paths for both gases are always greater than twice the diameter of the capillary tubes that form the array. This empirical rule of thumb, established by previous experimental investigations of the size and shape of molecular beams formed by effusive flow (Buckman *et al* 1993) along with the second requirement above, meant that the optimum ratio of driving pressures for the present measurements was $p(\mathrm{CO})/p(\mathrm{He}) = 0.48$ and the helium pressure was always around 1.0 Torr.

The measurements presented in this paper were carried out in two ways. Firstly, angular DCS were measured at a number of fixed energies between 1 and 30 eV. Under the experimental circumstances outlined above, and accompanied by careful measurements of electron beam currents and scattered signal rates, the application of the relative flow technique was made at each scattering angle and the resultant elastic differential cross sections for CO were determined with an uncertainty which varies between 6–10% depending on the contribution of statistical errors. The vibrational excitation cross sections were determined by measuring ratios of the inelastically scattered signal to the elastic, under conditions where the transmission of the electron spectrometer for the scattered electrons of different energy was optimized by scanning the analyser zoom lens voltages in sequence with the analyser energy loss voltage. In this work we have not measured the analyser transmission function though previous measurements and experience (Brunger *et al* 1990) lead us to believe that the assumption that it is uniform, over the small energy loss range covered here, is accurate to within 10% at an incident energy of 1 eV and better than 5% at

Table 1. (Continued.)

(*b*)	Energy (eV)					
Angle	5.0	6.0	7.5	9.9	20	30
10					7.60 (12)	10.616 (10)
15	1.956 (7)	2.028 (7)	2.314 (7)	2.813 (7)		
20	2.066 (7)	1.903 (7)	2.130 (7)	2.465 (7)	4.504 (7)	5.292 (7)
25	2.071 (7)	1.887 (7)	2.039 (7)	2.282 (7)	3.509 (7)	
30	2.113 (7)	1.911 (7)	1.947 (7)	2.079 (7)	2.569 (7)	2.544 (7)
35	2.119 (7)	1.911 (7)	1.871 (7)	1.958 (7)	2.015 (7)	
40	2.064 (7)	1.883 (7)	1.826 (7)	1.824 (7)	1.572 (7)	1.221 (7)
45	2.018 (7)	1.815 (7)	1.705 (7)	1.623 (7)	1.239 (7)	
50	1.896 (7)	1.720 (7)	1.606 (7)	1.464 (7)	0.995 (7)	0.636 (8)
55	1.777 (7)	1.598 (7)	1.455 (7)	1.314 (7)	0.788 (7)	
60	1.641 (7)	1.466 (7)	1.318 (7)	1.119 (7)	0.611 (8)	0.348 (7)
65	1.507 (7)	1.345 (7)	1.183 (7)	0.939 (7)		
70	1.312 (7)	1.176 (7)	1.006 (7)	0.774 (7)	0.383 (7)	0.208 (7)
75	1.175 (7)	1.029 (7)	0.861 (7)	0.625 (7)		
80	1.018 (7)	0.916 (7)	0.732 (7)	0.521 (7)	0.244 (7)	0.142 (7)
85	0.897 (7)	0.799 (7)	0.622 (7)	0.441 (7)		
90	0.798 (7)	0.710 (7)	0.543 (7)	0.391 (7)	0.222 (8)	0.123 (8)
95	0.715 (7)	0.628 (7)	0.486 (7)	0.382 (7)		
100	0.640 (7)	0.582 (7)	0.463 (7)	0.387 (7)	0.273 (7)	0.141 (7)
105	0.588 (7)	0.544 (7)	0.460 (7)	0.406 (7)		
110	0.565 (7)	0.528 (7)	0.465 (7)	0.440 (7)	0.362 (7)	0.199 (8)
115	0.538 (7)	0.526 (7)	0.488 (7)	0.484 (7)		
120	0.553 (7)	0.548 (7)	0.521 (7)	0.539 (7)	0.447 (7)	0.297 (8)
125	0.549 (7)	0.564 (7)	0.560 (7)	0.575 (7)		
130	0.553 (7)	0.590 (7)	0.607 (7)	0.624 (7)	0.554 (7)	0.441 (7)
σ_E	14.0	12.9	12.0	11.4	11.0	10.3
σ_M	10.3	9.8	8.9	8.3	6.6	5.6

energies above 5 eV. As a result the uncertainties on the differential vibrational excitation cross sections vary between 10 and 20%.

The second technique we have employed was to measure the energy dependence (excitation function) for both elastic scattering and rovibrational excitation at two fixed scattering angles and over an energy range (1–6 eV) encompassing the shape resonance. These measurements were also placed on an absolute scale by use of the relative flow technique. At each angle, the yield of scattered electrons as a function of energy, in 20 meV steps, was measured for both He and CO elastic scattering, CO inelastic ($\nu = 0$–1) scattering and the elastic and inelastic background. In addition, the electron current at each energy was also measured and used to normalize the scattered signal levels. The measurements were carried out under computer control and the monochromator and analyser zoom lens voltages were varied in conjunction with the incident energy in order to maintain optimum transmission of the electron optics. The sequence of He, CO, and background measurements was cycled continuously to minimize the effects of any short-term drifts in the apparatus. The final spectra represent weighted sums of many individual measurements and the excitation functions obtained in this fashion have estimated uncertainties of $\pm 15\%$ for the elastic channel and $\pm 20\%$ for the vibrationally inelastic channel.

3. Theoretical considerations

At energies below 5 eV the theoretical differential cross sections were obtained from the *R*-matrix model described by Morgan (1991). This model employed a simple SCF wavefunction to describe the target molecule whilst the non-adiabatic formalism of Schneider *et al* (1979) was used to describe the vibrational motion.

At higher energies, the more sophisticated *R*-matrix model of Morgan and Tennyson (1993) was used to calculate the differential cross sections. This differs from the earlier approach primarily in that eight target states were included and all were represented by more sophisticated CI wavefunctions. The correlation terms added to the wavefunction for the whole system of target molecule plus scattered electron were chosen to give a good representation of the collision process for energies in the range of 5–15 eV. They had the additional, unwanted effect of slightly over-correlating the 2 eV $^2\Pi$ resonance state compared to the ground state and as a result the present low energy measurements have been compared with the earlier calculation.

Conversely the earlier one-state model is inappropriate at energies close to and above the threshold for excitation of the a $^3\Pi$ electronic state and the more recent theory has thus been used in these cases, in conjunction with an adiabatic nuclei approach.

4. Results and discussion

4.1. Elastic scattering

Experimental absolute differential cross sections for elastic scattering at 13 incident energies between 1.0 and 30 eV are given in table 1. Comparisons with other experimental results and with the present theoretical calculations are made in figures 1–3. In figure 1(*a*)–(*e*) we show a comparison at energies of 1.0, 1.50, 1.91, 2.45 and 3.0 eV. The measurements at 1.91 and 2.45 eV correspond to the positions of resonance structures which can be clearly identified in the vibrational ($\nu = 0$-1) excitation channel.

At 1 eV (figure 1(*a*)) we can compare the present results with the relative angular distributions of Ehrhardt *et al* (1968) which we have normalized to the present data at a scattering angle of 90°. Whilst there is very good agreement between the shapes of the two cross sections there are large discrepancies between these measurements and both the Born-dipole approximation cross section and the present *R*-matrix calculation based on the approach of Morgan (1991). A similar comparison is made at 1.5 eV (figure 1(*b*)), where the normalization was made at 60°, and again the level of agreement between the shape of the experimental cross sections is reasonable although there are some differences (20–30%) at both forward and backward angles. Once again there are substantial differences with the *R*-matrix calculation at this energy, probably due to the lack of polarization effects in the theoretical model which will be more significant at very low energies where the contribution from the non-resonant $^2\Sigma^+$ symmetry dominates the cross section. Similar discrepancies, between theory and experiment on the low energy side of a resonance have also been observed in the case of N_2 (Gillan *et al* 1987).

At energies between 1.5 and about 3 eV, both elastic scattering and vibrational excitation are enhanced by the formation of a temporary negative ion of $^2\Pi$ symmetry. This resonance has an intermediate lifetime such that in certain decay channels there is evidence for narrow and weak quasi-vibrational structure superimposed on a broad resonance structure. In the elastic channel these features are extremely weak and represent only a few per cent of the overall resonant plus direct scattering cross section. In the vibrational ($\nu = 0$-1) channel

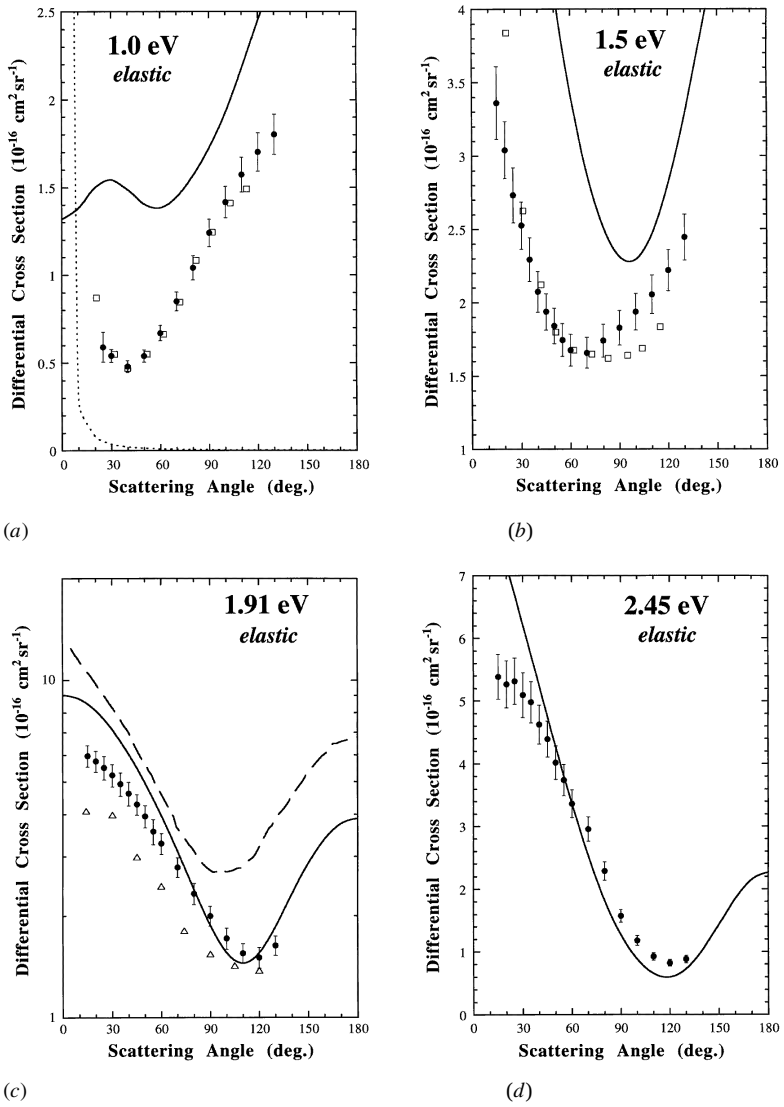

Figure 1. Differential cross sections (10^{-16} cm^2 sr^{-1}) for elastic electron scattering from CO at energies of (*a*) 1.0 eV, present data (●), Ehrhardt *et al* (□) normalized to the present data at 90°, Born-dipole approximation (– – –), present theory (——); (*b*) 1.5 eV, present data (●), Ehrhardt *et al* (□) 1.45 eV, normalized to the present data at 60°, present theory (——); (*c*) 1.91 eV, present data (●), Jung *et al* (△), 1.83 eV Jain and Norcross (— — —), 1.83 eV, present theory (——); (*d*) 2.45 eV, as above; (*e*) 3.0 eV, present data (●), Tanaka *et al* (○), Jain and Norcross (— — —), present theory (——).

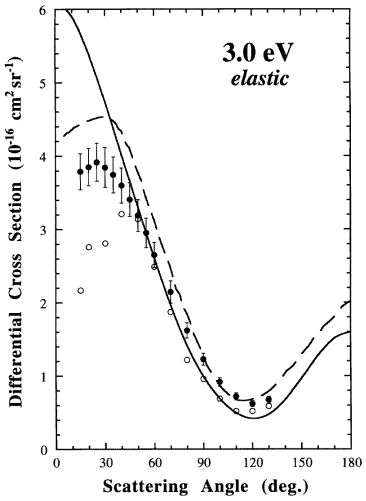

(*e*)

Figure 1. Continued.

they appear at about the 10–20% level of the broad resonant background and their positions are easily identifiable with moderate energy resolution. The details of these determinations are presented in the next section but we have carried out a number of DCS measurements at the positions of resonance structures as determined in the vibrational excitation channel. These particular structures were found, at a scattering angle of 60°, at energies of 1.91 and 2.45 eV, and the DCS measurements at these energies are shown in figures 1(*c*) and (*d*) respectively. With the exception of small differences in absolute magnitude there are no significant differences in the shape of the two cross sections. At 1.91 eV we can compare the present experiment with a previous measurement made at an energy of 1.83 eV, but apparently coinciding with the same resonance feature, by Jung *et al* (1982). The present measurement is uniformly higher in magnitude across the entire angular range by between $10 - 30\%$ but there is good general agreement as to the shape of the DCS. A similar conclusion can be drawn from the comparison with the theoretical calculations of Jain and Norcross (1992) and the present *R*-matrix theory, both of which show similar angular behaviour to the experiment. The calculation of Jain and Norcross is uniformly larger in magnitude than the present experiment whilst the *R*-matrix cross section is larger for scattering angles less than about 80°, but in reasonably good agreement with the present experiment beyond that. At 2.45 eV there is good overall agreement between the present experiment and *R*-matrix theory except at the most forward angles where the theoretical magnitude is substantially larger.

At an energy of 3 eV, on the high energy tail of the resonance, there is a slight change in the angular behaviour of the cross section with the DCS decreasing at angles below about 30° (figure 1(*e*)). A similar, but slightly displaced, shape is observed in the cross section of Tanaka *et al* (1978) and there is fair agreement between the magnitude of the present cross section and that of Tanaka *et al* at angles above about 50°. Below this angle the present experimental cross section is substantially larger. Theories in general agree well with the present measurements although that of Jain and Norcross appears to have a closer level of agreement in shape whilst the present calculation does not show the decrease in the DCS at forward angles. This decrease at forward scattering angles in this energy region has been

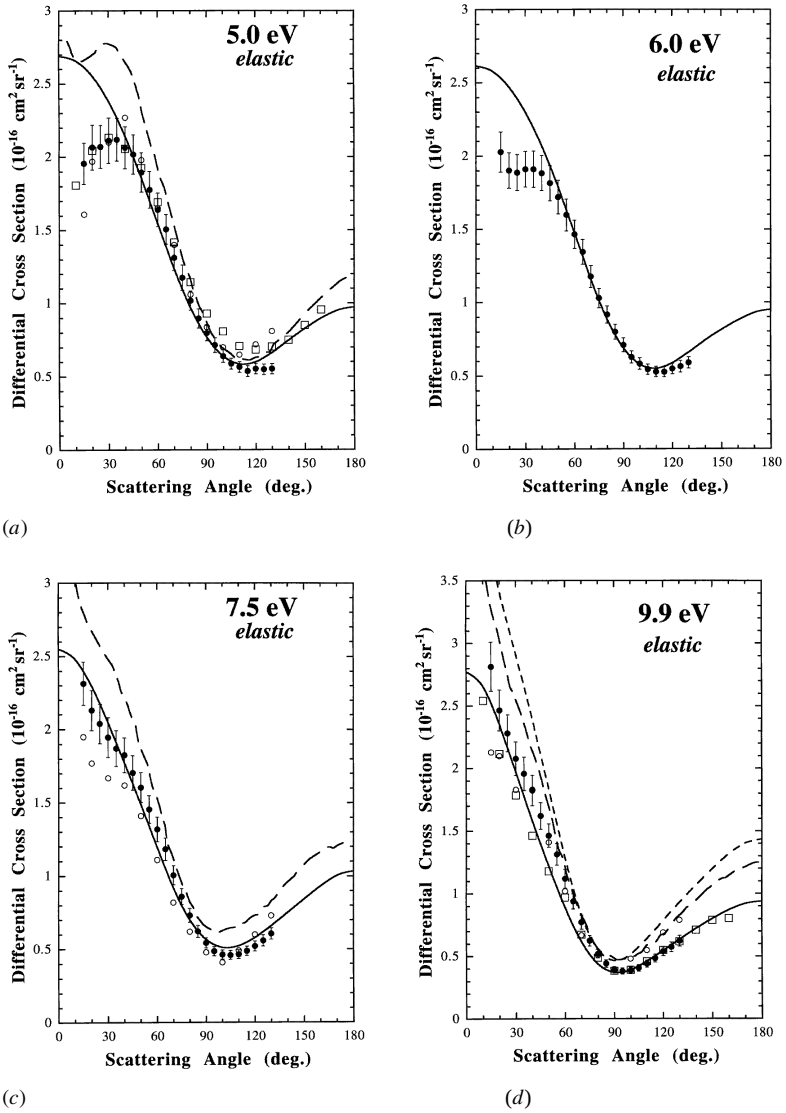

Figure 2. Differential cross sections (10^{-16} cm^2 sr^{-1}) for elastic electron scattering from CO at energies of (*a*) 5.0 eV, present data (●), present theory (——), Tanaka *et al* (○), Jain and Norcross (— — —), Gote *et al* (□); (*b*) 6.0 eV, present data (●), present theory (——); (*c*) 7.5 eV, present data (●), present theory (——), Tanaka *et al* (○), Jain and Norcross (— — —); (*d*) 9.9 eV, present data (●), present theory (——), Tanaka *et al* (○), Jain and Norcross (— — —), Gote *et al* (□), Onda and Truhlar (– – –).

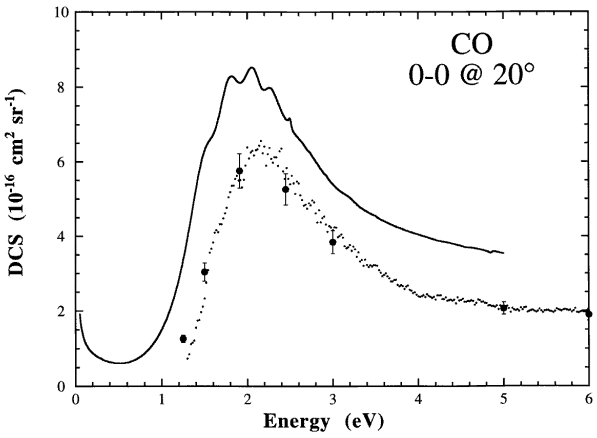

(*a*)

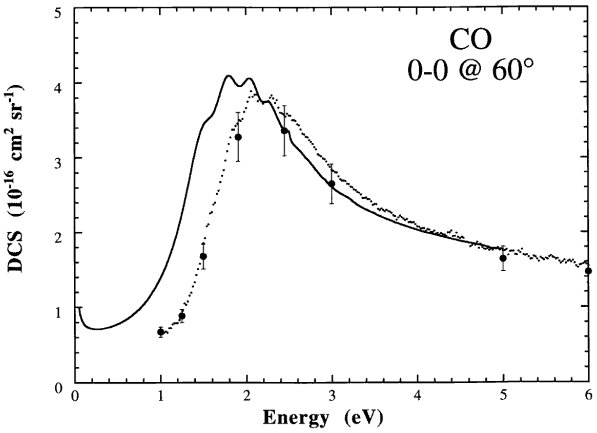

(*b*)

Figure 3. Energy dependence of the elastic differential cross section between 1 and 6 eV at a scattering angle of (*a*) 20° and (*b*) 60°. Present experimental results: excitation function technique (· · · · · ·), angular DCS measurements (●), present theory (——).

noted, and commented upon, for several other molecules (e.g. Gibson *et al* 1995, Sun *et al* 1995).

In figure 2(*a*) we give a comparison of the present measurements at an energy of 5.0 eV with the experiments of Tanaka *et al* and Gote and Ehrhardt (1995), the present calculation and that of Jain and Norcross. With the exception of the most backward angles (above about 100°), where the present measurement is smaller in magnitude than both the others, the three experiments are in exceptionally good agreement and all indicate a strong turnover of the cross section at forward angles. This behaviour is also evident in the calculation of Jain and Norcross which is, however, larger than all three experiments for scattering angles less than 90°. The present *R*-matrix calculation, based on the formalism of Morgan and Tennyson (1993), is in excellent agreement with the experiments between 40–130° but once again does not show the turnover in the cross section at forward angles (< 30°). At 6.0 eV (figure 2(*b*)) the experimental DCS has changed shape again with the decrease in the

cross section at forward angles, which was evident at lower energies, having developed into a plateau in the region around 20–40° with a subsequent increase at smaller angles. Once again the *R*-matrix calculation does not reproduce these subtle details at forward angles but the agreement above 40° is excellent.

At 7.5 eV (figure 2(*c*)) there is once again quite good agreement between the present measurements and those of Tanaka *et al* , particularly at angles greater than 50°. Below this, both cross sections indicate some subtle angular structure although the present measurements are consistently larger in magnitude by 20–30%. Whilst the *R*-matrix calculation does not reproduce these subtle variations at forward angles it does an excellent job at predicting the overall shape and magnitude of the cross section. The calculated cross section of Jain and Norcross is also in good agreement with the shape of the DCS although typically 20–40% larger in magnitude. In figure 2(*d*) we compare the present measurements and *R*-matrix cross section at an energy of 9.9 eV with the experiments of Tanaka *et al* (also at 9.9 eV) and Gote and Ehrhardt and the calculations of Jain and Norcross and Onda and Truhlar, all of which were done at 10 eV. The energy of 9.9 eV was chosen in the present measurement and theory in order to avoid the possible complication of comparison near the sharp $^2\Sigma^+$ Feshbach resonance at 10.04 eV (Newman *et al* 1983). The agreement between the present experimental result and that of Tanaka *et al* is good in the mid-angle range although there are substantial discrepancies at both forward and backward angles. In contrast to the situation at 5 eV, the cross section of Gote and Ehrhardt lies below the present (by about 20%) at angles less than 80° but is in excellent agreement at larger angles. In general the present experiment and theory are in good agreement across most of the angular range, the theory also being in good accord with the data of Gote and Ehrhardt. There is also good agreement in shape between the present data and the calculations of Jain and Norcross and Onda and Truhlar, although both of these calculations are somewhat higher in magnitude at all angles.

For reasons of brevity we do not depict the elastic DCS for 20 and 30 eV but it is worth noting that the level of agreement between the present measurements and those of Nickel *et al* (1988) and Middleton *et al* (1993) is excellent at both of these energies. On the other hand the data of Tanaka *et al* are lower in magnitude by between 10 and 40% across the entire angular range at both energies.

In figures 3 (*a*) and (*b*) we show the energy dependence of the absolute elastic differential cross section between 1 and 6 eV and at scattering angles of 20° and 60° respectively. The broad $^2\Pi$ shape resonance, centred at about 2.2 eV, is clearly evident, enhancing the non-resonant background cross section by between a factor of two and three and with a width of around 2 eV. Also shown on these curves for comparison are the individual DCS measurements from the angular scans, which have a smaller absolute uncertainty, but which are in good agreement with the excitation function values. Near the peak in the experimental cross section, particularly at an angle of 60°, there is evidence of weak quasi-vibrational resonance structures at energies of 1.90 eV, 2.06 eV and 2.30 eV. The results of the present theory are also shown and, whilst they exhibit remarkably similar structures in the cross section, these features are shifted to lower energies by about 0.2 eV.

4.2. Vibrational excitation

Absolute differential cross sections for vibrational excitation ($v = 0 - 1$) of CO at energies between 1.0 and 3.0 eV, i.e. within the resonance region, and at 20 and 30 eV are given in table 2. A comparison between the present experimental results and theory and other experiment and theory is given in figures 4–6. In figures 4(*a*)–(*f*) the results encompass the $^2\Pi$ resonance region and the measurements at 1.91 eV (figure 4(*d*)) and 2.45 eV (figure

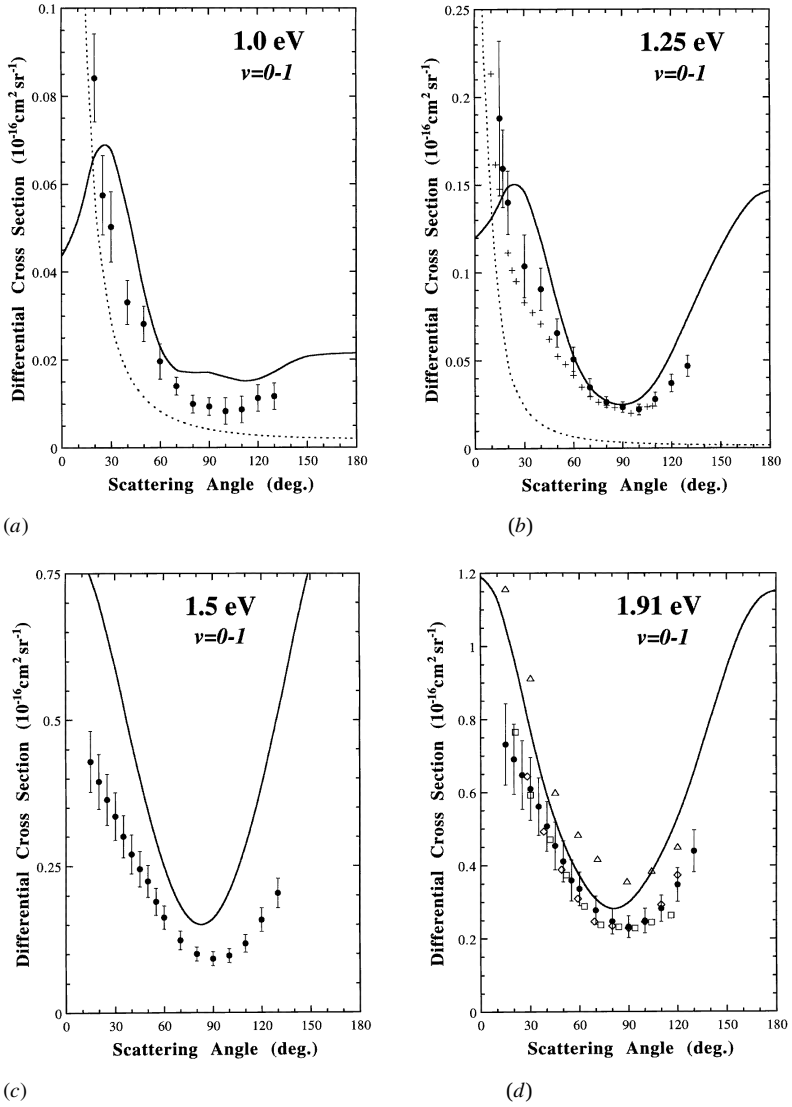

Figure 4. Differential cross sections (10^{-16} cm^2 sr^{-1}) for vibrational excitation ($v = 0$–1) of CO at (*a*) 1.0 eV, present data (●), Born-dipole approximation (– – –), present theory (——); (*b*) 1.25 eV, present data (●), Sohn *et al* (+), Born-dipole approximation (– – –), present theory (——); (*c*) 1.5 eV, present data (●); present theory (——); (*d*) 1.91 eV, present data (●), present theory (——), Ehrhardt *et al* (□) normalized to the present data at 90°, Tronc *et al* (◊) normalized to the present data at 90°, Jung *et al* (△) 1.83 eV; (*e*) 2.45 eV, present data (●), present theory (——), Ehrhardt *et al* (□) normalized to the present data at 90°; (*f*) 3.0 eV, current data (●), present theory (——), Ehrhardt *et al* (□) normalized to the present data at 90°, Chutjian and Tanaka (○).

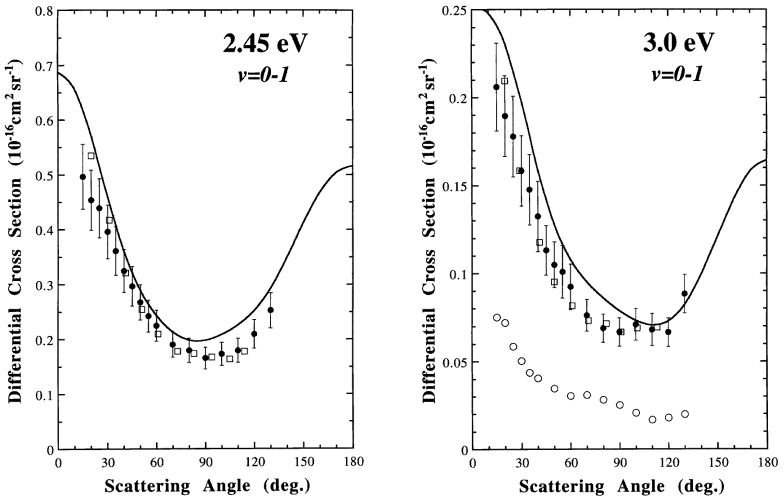

(*e*) (*f*)

Figure 4. Continued.

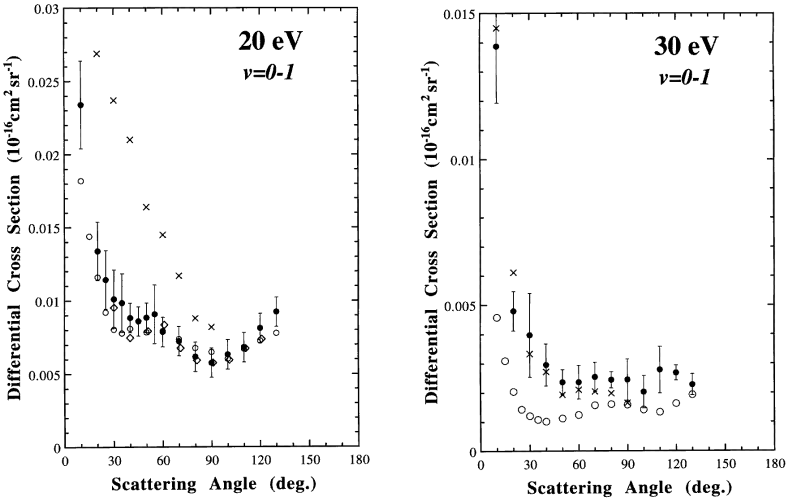

(*a*) (*b*)

Figure 5. Differential cross sections (10^{-16} cm^2 sr^{-1}) for vibrational excitation ($v = 0$–1) of CO at (*a*) 20 eV, present data (●), Tronc *et al* (◊) at 19.5 eV, normalized to the present data at 90°, Chutjian and Tanaka (○), Middleton *et al* (×); (*b*) 30 eV, present data (●), Chutjian and Tanaka (○), Middleton *et al* (×).

4(*e*)) correspond to the energies at which two resonance peaks occur in the vibrational excitation function at a scattering angle of 60° (see previous section).

At an energy of 1.0 eV (figure 4(*a*)), which is below the dominant influence of the resonance, the magnitude of the cross section is small but increasing strongly at the more forward scattering angles, a consequence of the direct dipole scattering. Indeed at small angles the DCS appears to approach both the shape and magnitude predicted by the Born-

(*a*)

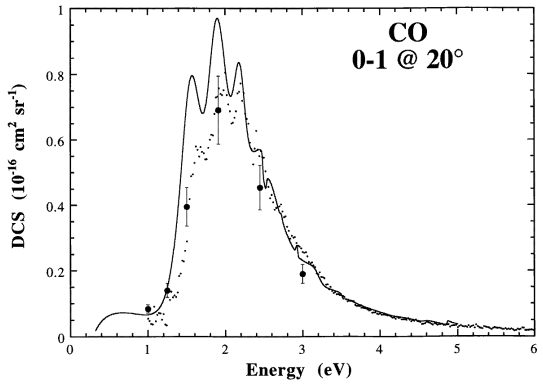

(*b*)

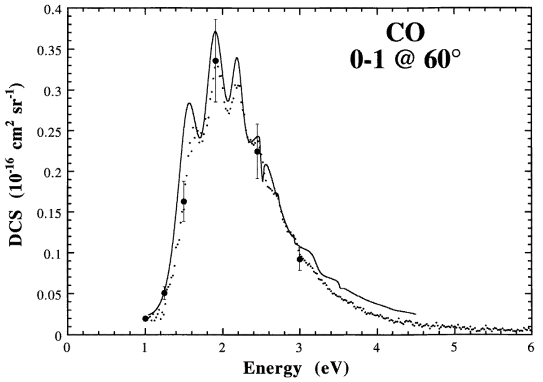

Figure 6. Energy dependence of the $v = 0$–1 differential cross section between 1 and 6 eV at a scattering angle of (*a*) 20° and (*b*) 60°. Present experimental results: excitation function technique (· · · · · ·) angular DCS measurements (●); present theory (——).

dipole approximation. The present *R*-matrix calculation gives a reasonable description of the DCS at large scattering angles ($> 50°$) but shows the opposite behaviour to that observed experimentally at small angles. The lowest energy at which we can compare the present and previous experiments is 1.25 eV (figure 4(*b*)), where there is generally good agreement with the result of Sohn *et al* (1985) although the present result appears to be uniformly higher by between 5–20%. Once again the current theory is in good agreement with experiment only at scattering angles greater than 60°. By 1.5 eV (figure 4(*c*)) the magnitude of the cross section has grown considerably under the influence of the resonance and the level of agreement with the *R*-matrix theory is worse. This is probably due to the fact that the cross section is increasing rapidly near this energy and so small differences in the resonance position will have a disproportionate effect on any comparisons of magnitudes. The failure of the theory to predict the low angle behaviour for these low energy inelastic cross sections can be attributed to the truncation in the angular momentum expansion. The dipole potential couples all *l*-values and, since this is the dominant potential at very low energies, a model which avoids the partial wave expansion, such as the Born-dipole approximation, will do better in this regime.

At the position of the maximum in the vibrational excitation cross section (1.91 eV in the current work) several other experimental cross sections are available for comparison and these are shown in figure 4(*d*). Two of these are relative measurements (Ehrhardt *et al* and

Table 2. Absolute differential cross sections (10^{-16} cm^{2}sr^{-1}) for vibrational excitation of CO ($v = 0$–1) between 1.0 and 30 eV. Numbers in parentheses indicate the absolute uncertainty of the present measurements expressed as a percentage. Integral cross sections σ_v are given in units of 10^{-16} cm^2 with an estimated uncertainty of ±20%.

	Energy (eV)							
Angle	1.0	1.25	1.50	1.91	2.45	3.0	20	30
10							0.023 (14)	0.014 (16)
15		0.188 (23)	0.429 (12)	0.732 (15)	0.497 (12)	0.206 (12)		
17		0.159 (14)						
20	0.084 (12)	0.140 (13)	0.395 (12)	0.691 (14)	0.454 (12)	0.190 (12)	0.013 (13)	0.0048 (16)
25	0.057 (16)		0.364 (12)	0.648 (14)	0.439 (12)	0.178 (13)	0.011 (16)	
30	0.050 (17)	0.104 (17)	0.335 (12)	0.610 (14)	0.396 (12)	0.158 (13)	0.010 (17)	0.0040 (36)
35			0.300 (12)	0.561 (14)	0.361 (12)	0.148 (14)	0.0098 (20)	
40	0.033 (16)	0.091 (13)	0.270 (12)	0.507 (13)	0.325 (12)	0.132 (15)	0.0088 (16)	0.0030 (29)
45			0.245 (12)	0.454 (14)	0.297 (12)	0.113 (13)	0.0086 (15)	
50	0.028 (14)	0.066 (13)	0.224 (12)	0.411 (14)	0.268 (12)	0.105 (13)	0.0088 (14)	0.0024 (18)
55			0.190 (12)	0.359 (16)	0.242 (12)	0.101 (15)	0.0091 (17)	
60	0.020 (18)	0.051 (14)	0.163 (12)	0.336 (14)	0.225 (12)	0.092 (14)	0.0079 (14)	0.0024 (24)
70	0.014 (19)	0.035 (14)	0.124 (12)	0.278 (14)	0.191 (12)	0.076 (12)	0.0072 (15)	0.0025 (20)
80	0.0099 (22)	0.026 (13)	0.100 (12)	0.247 (14)	0.180 (12)	0.069 (12)	0.0062 (18)	0.0024 (15)
90	0.0094 (18)	0.023 (14)	0.092 (13)	0.233 (13)	0.166 (12)	0.067 (12)	0.0058 (13)	0.0025 (29)
100	0.0083 (31)	0.022 (15)	0.097 (12)	0.249 (14)	0.174 (12)	0.071 (12)	0.0063 (17)	0.0020 (27)
110	0.0087 (37)	0.028 (15)	0.118 (12)	0.283 (13)	0.180 (13)	0.068 (14)	0.0068 (16)	0.0028 (29)
120	0.011 (28)	0.037 (14)	0.158 (13)	0.347 (13)	0.210 (12)	0.067 (12)	0.0081 (16)	0.0027 (14)
130	0.012 (23)	0.047 (14)	0.204 (12)	0.439 (13)	0.253 (13)	0.088 (12)	0.0092 (13)	0.0023 (18)
σ_v	0.24	0.65	2.4	4.9	3.1	1.2	1.1	0.035

Tronc *et al*) and they have both been normalized to the present measurements at a scattering angle of 90°. In both cases the agreement of the present data with the shape of these cross sections is excellent. This is also the case with the absolute measurements of Jung *et al* although the present cross section is about 30–40% smaller across the entire angular range. The agreement between the present experimental and theoretical cross section at this energy is fair. At 2.45 eV (figure 4(*e*)), an energy which corresponds to a higher quasi-vibrational resonance peak in our vibrational excitation cross section, there is good overall agreement between the shape of the present cross section and that of Ehrhardt *et al* and with the present *R*-matrix theory. A similar comment applies to our final comparison within the resonance region at an energy of 3 eV (figure 4(*f*)). However, at this energy we can also compare, for the first time, with the measurements of Chutjian and Tanaka which show a similar shape to the present data but are more than a factor of two lower in absolute magnitude.

At higher energies, vibrational excitation in CO is significantly affected by a further, broad resonance centred at 19.5 eV which has been classified as a σ shape resonance with a dominant f-wave angular distribution (Tronc *et al* 1980). Our measurements of the DCS at 20 eV (figure 5(*a*)) are in complete accord with this and also show good agreement in absolute magnitude with the results of Chutjian and Tanaka. However the agreement with the most recent measurements of Middleton *et al* (1992) is poor with these latter results showing essentially no influence of the shape resonance on the angular distribution. We note that as the present elastic DCS at this energy is in good accord with that of Middleton *et al* this discepancy must be the result of a difference in the measured ratio of elastic to inelastic scattering in the two experiments. At 30 eV (figure 5(*b*)), above the influence

of the σ shape resonance, the situation is reversed with the present results showing good agreement with those of Middleton *et al*, both in shape and absolute magnitude. Both of these measurements are substantially larger than the cross section of Chutjian and Tanaka at most scattering angles.

The energy dependence of the absolute vibrational (0–1) excitation cross section in the region of the $^2\Pi$ resonance is shown in figures 6(*a*) and (*b*) for scattering angles of 20° and 60° respectively. At both these angles the $^2\Pi$ resonance dominates the $\nu = 0 - 1$ cross section, enhancing the small, non-resonant component of the cross section by more than a factor of thirty. In this case the resonance is centred at around 1.9 eV and once again shows a width of around 1.5 eV. The quasi-vibrational features are also better developed in this channel, representing about 15–20% of the broad cross section feature. At an angle of 60° the dominant structures occur at energies of 1.65, 1.91, 2.20 and 2.45 eV, which are both different energies and separations to that exhibited in the elastic channel at the same scattering angle (figure 3(*b*))—an indication of the 'boomerang' nature of this resonance. There is no significant difference in the positions of the resonance peaks at these two scattering angles in the 0–1 channel. Also shown in figures 6(*a*) and (*b*) are the absolute cross sections obtained from the individual angular DCS measurements, which are in excellent agreement with the excitation function values, and the cross section from the present *R*-matrix calculation which is also in remarkably good agreement with the experiment, particularly at 60°, both in terms of the magnitude and the positions of the dominant features of the cross section.

4.3. Integral cross sections

The present experimental differential cross sections for elastic scattering and vibrational excitation have been extrapolated to forward and backward angles and integrated to yield integral elastic, elastic momentum transfer and integral vibrational (ν = 0-1) excitation cross sections.

The integral elastic cross section is compared, in figure 7, with the integral elastic cross sections of Tanaka *et al* (1978) and Nickel *et al* (1988) which were deduced from their elastic DCS measurements, and a recommended integral elastic cross section which has been deduced by Kanik *et al* (1993) and with the theoretical results of Onda and Truhlar (1980), Jain and Baluja (1992) and Jain *et al* (1984). There is good agreement between the present experimental cross section and the recommended values of Kanik *et al* (1993) particularly at energies above the resonance peak. There is also good agreement between the present values and those of both Tanaka *et al* and Nickel *et al*. The calculation of Jain and Baluja clearly overestimates the magnitude of the cross section between 10 and 40 eV whilst at 10 eV the calculation of Onda and Truhlar is about 30% higher than the experiments.

For the momentum transfer cross section, comparison can be made between the present experiment, the DCS-derived values of Tanaka *et al* (1978) and the swarm measurements of Haddad and Milloy (1983). Calculated results have been reported by Jain and Norcross (1992) and Jain *et al* (1984). These data are illustrated in figure 8. At energies above and below the resonance peak, the present data are in fair agreement with those of Haddad and Milloy, whilst in the region of the resonance peak the present results are about 50% lower than the swarm cross section. Some of this difference may be explained by the fact that the swarm result is not the elastic momentum transfer cross section but also includes inelastic (rotational and vibrational) processes. Once again the present results are in good agreement with the cross sections of Tanaka *et al*. The calculation of Jain and Norcross is in good general agreement with both the cross section of Haddad and Milloy and the present. The

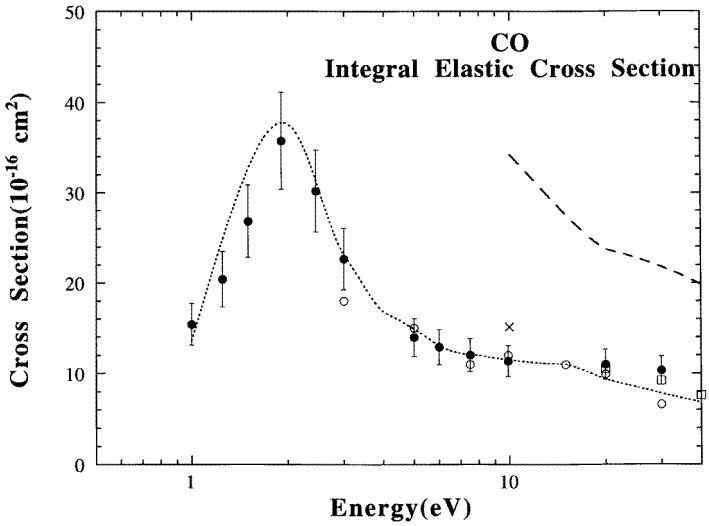

Figure 7. Integral elastic scattering cross section (10^{-16} cm^2) for CO. Present data (●), Tanaka *et al* (○), Nickel *et al* (□); Kanik *et al* (- - - -); Onda and Truhlar (×); Jain and Baluja (– – –).

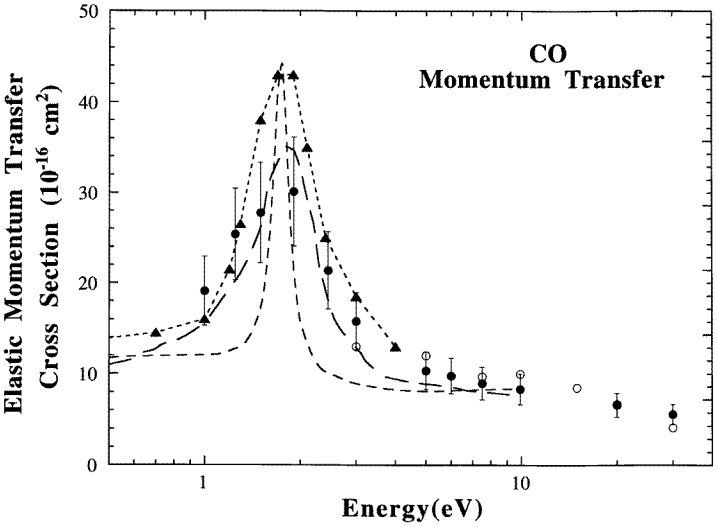

Figure 8. Elastic momentum transfer cross section (10^{-16} cm^2) for CO. Present data (●), Tanaka *et al* (○), Haddad and Milloy (– ▲–), Chandra (- - - -), Jain and Norcross (— — —).

calculation of Chandra (1977) shows a strong, narrow shape resonance whose position and magnitude is in good agreement with the swarm result and, to a slightly lesser extent, the present cross section. The width of this feature is however substantially narrower than is evident in both experiments.

Experimental integral vibrational excitation ($v = 0$-1) cross sections for CO have been reported by Sohn *et al* (1985), Land (1978) and Chutjian and Tanaka (1980). Theoretical

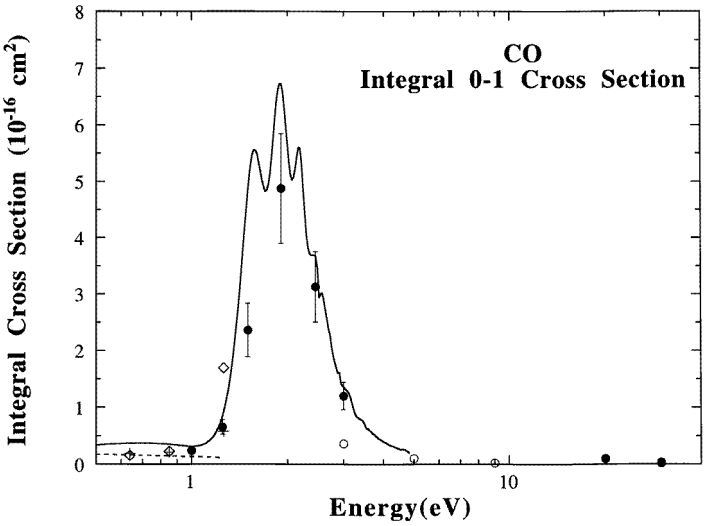

Figure 9. Integral cross section for vibrational excitation (0–1) of CO (10^{-16} cm^2). Present data (●), Chutjian and Tanaka (○), Sohn *et al* (+), Land (◇), present theory (——), Born-dipole approximation (– – –).

calculations include the present *R*-matrix formalism, while at very low energies Born dipole approximation results are also available (Sohn *et al* 1985). All the presently available experimental data and theoretical calculations are shown in figure 9. It is apparent that there is not a great deal of overlap in the energy range covered by the various experimental determinations. Where overlap does exist, agreement between the various cross sections is only marginal. At energies below the resonance the present data and those of Sohn *et al* and Land appear to be in fair accord. In general the cross section of Chutjian and Tanaka is smaller in magnitude than the present, consistent with what is observed in the DCS comparisons. The present *R*- matrix calculation is in reasonable agreement with the present data in the resonance region.

5. Conclusions

The present experimental and theoretical investigation of low energy elastic electron scattering and vibrational excitation of CO provides a substantial body of absolute scattering data and *R*-matrix calculations, over a wide range of incident energies which can be critically compared, both against each other and with previous measurements and theory, particularly at energies in and around the $^2\Pi$ resonance. These comparisons clearly indicate the need for additional theoretical studies at an *ab initio* level for both elastic scattering and $\nu = 0$-1 vibrational excitation at energies below about 1.5 eV. There is also an almost complete absence of calculations in both the elastic and vibrational excitation channels for incident energies above 20 eV. Furthermore the interesting forward angle behaviour of the elastic DCS for incident energies between 2.5 and 7.5 eV could benefit from further theoretical clarification.

We note that in some sense the present integral cross section for the $\nu = 0$-1 excitation fills an important gap in the literature. This is particularly true for studies such as that by

Liu and Victor (1994) who attempted to model the electron energy deposition in CO gas, but who experienced difficulties due to the limited availability of experimental total cross section data.

Acknowledgments

It is a pleasure to acknowledge once again the skill and craftsmanship of the technical staff of the Electron Physics Group for their assistance in maintaining the apparatus in an operational form. JCG is grateful to the ANU Graduate School for the provision of a scholarship, MJB acknowledges both the ANU and Flinders University for support under the Institute of Advanced Studies (ANU)–Flinders University Collaborative Research Program and CTB the support of the Friedrich Ebert Stiftung, Germany, for the provision of a Scholarship.

References

Brunger M J, Buckman S J and Newman D S 1990 *Aust. J. Phys.* **43** 665
Buckman S J, Gulley R J, Moghbelalhossein M and Bennett S J 1993 *Meas. Sci. Technol.* **4** 1143
Chandra N 1977 *Phys. Rev.* A **16** 80
Chutjian A and Tanaka H 1980 *J. Phys. B: At. Mol. Phys.* **13** 1901
Ehrhardt H, Langhans L, Linder F and Taylor H S 1968 *Phys. Rev.* **173** 222
Gibson J C, Sullivan J P, Gulley R J, Brunger M J and Buckman S J 1995 *XIXth Int. Conf. on the Physics of Electronic and Atomic Collisions* (New York: Whistler) Abstracts p 6
Gillan C J, Nagy O, Burke P G, Morgan L A and Noble C J 1987 *J. Phys. B: At. Mol. Phys.* **20** 4585
Gote M and Ehrhardt H 1995 *J. Phys. B: At. Mol. Opt. Phys.* **28** 3957
Gulley R J, Alle D T, Brennan M J, Brunger M J and Buckman S J 1994 *J. Phys. B: At. Mol. Opt. Phys.* **27** 2593
Haddad G N and Milloy H B 1983 *Aust. J. Phys.* **36** 473
Jain A and Baluja K L 1992 *Phys. Rev.* A **45** 202
Jain A, Freitas L C G, Mu-Tao L and Tayal S S 1984 *J. Phys. B: At. Mol. Phys.* **17** L29
Jain A and Norcross D W 1992 *Phys. Rev.* A **45** 1644
Jung K, Antoni T, Müller R, Kochem K-H and Ehrhardt H 1982 *J. Phys. B: At. Mol. Phys.* **15** 3535
Kanik I, Trajmar S and Nickel J C 1993 *J. Geophys. Res.* **98** 7447
Land J E 1978 *J. Appl. Phys.* **49** 5716
Liu W and Victor G A 1994 *Harvard-Smithsonian Centre for Astrophysics* Reprint Series 3872, 1
Middleton A G, Brunger M J and Teubner P J O 1992 *J. Phys. B: At. Mol. Opt. Phys.* **25** 3541
——1993 *J. Phys. B: At. Mol. Opt. Phys.* **26** 1743
Morgan L A 1991 *J. Phys. B: At. Mol. Opt. Phys.* **24** 4649
Morgan L A and Tennyson J 1993 *J. Phys. B: At. Mol. Opt. Phys.* **26** 2429
Newman D S, Zubek M and King G C 1983 *J. Phys. B: At. Mol. Phys.* **16** 2247
Nickel J C, Mott C, Kanik I and McCollum D C 1988 *J. Phys. B: At. Mol. Opt. Phys.* **21** 1867
Nickel J C, Zetner P W, Shen G and Trajmar S 1989 *J. Phys. E: Sci. Instrum.* **22** 730
Onda K and Truhlar D G 1980 *J. Phys. C: Solid State* **72** 5249
Reid R C, Prausnitz J M and Poling B E 1987 *The Properties of Gases and Liquids* (New York: McGraw-Hill)
Rohr K 1977 *J. Phys. B: At. Mol. Phys.* **10** 2215
Salvini S, Burke P G and Noble C J 1984 *J. Phys. B: At. Mol. Phys.* **17** 2549
Schneider B, Le Dourneuf M and Burke P G 1979 *J. Phys. B: At. Mol. Phys.* **12** L365
Sohn W, Kochem K-H, Jung K, Ehrhardt H and Chang E S 1985 *J. Phys. B: At. Mol. Phys.* **18** 2049
Sun W, Morrison M A, Isaacs W A, Trail W K, Alle D T, Gulley R J, Brennan M J and Buckman S J 1995 *Phys. Rev.* A **52** 1229
Tanaka H, Srivastava S K and Chutjian A 1978 *J. Chem. Phys.* **69** 5329
Tronc M, Azria R and Le Coat Y 1980 *J. Phys. B: At. Mol. Phys.* **13** 2327